Graphene Optomechanics Realized at Microwave Frequencies

X. Song,[1] M. Oksanen,[1] J. Li,[1] P. J. Hakonen,[1] and M. A. Sillanpää[1,2*]
[1]O. V. Lounasmaa Laboratory, Low Temperature Laboratory, Aalto University, P.O. Box 15100, FI-00076 Aalto, Finland.
[2]Department of Applied Physics, Aalto University School of Science, P.O. Box 11100, FI-00076 Aalto, Finland
(Received 13 March 2014; published 11 July 2014)

Cavity optomechanics has served as a platform for studying the interaction between light and micromechanical motion via radiation pressure. Here we observe such phenomena with a graphene mechanical resonator coupled to an electromagnetic mode. We measure thermal motion and backaction cooling in a bilayer graphene resonator coupled to a microwave on-chip cavity. We detect the lowest flexural mode at 24 MHz down to 60 mK, corresponding to 50 ± 6 mechanical quanta, which represents a phonon occupation that is nearly 3 orders of magnitude lower than that which has been recorded to date with graphene resonators.

DOI: 10.1103/PhysRevLett.113.027404 PACS numbers: 78.67.Wj, 42.50.Ct, 62.25.-g, 72.80.Vp

Graphene can be considered as an ultimate material for studying the quantum behavior of the motion of micromechanical resonators. It is lightweight, and therefore the zero-point motion $x_{\mathrm{zp}} = \sqrt{\hbar/2m_{\mathrm{eff}}\omega_m}$ of a particular mode of frequency ω_m and effective mass m_{eff} is unusually large. It is stiff, such that the frequency is high for a given mass, allowing for approaching the quantum limit in dilution refrigerator temperatures. These properties would make graphene attractive for the use in cavity optomechanics experiments.

In the field of cavity optomechanics [1], remarkable findings have been made during the last ten years. These include, for example, ground-state cooling of a mechanical mode [2,3]. Briefly, an optical or more generally electromagnetic cavity mode with a movable mirror or boundary condition allows one to couple the confined photons and the motion by means of the radiation pressure exerted by the photons.

Photothermal interaction between the motion of a mechanical resonator made with graphene [4–7] and light was observed quite recently [8]. These authors had an on-chip trench covered by graphene, thus forming the cavity. However, since the graphene end mirror is 98% transparent, the Q value was much less than 1, and canonical radiation pressure phenomena could not be observed.

In contrast to optical frequencies, graphene naturally lends itself to microwave-frequency cavities as it is opaque to the electric field which dominates in a plate capacitor geometry at these frequencies. The driven motion of a graphene mechanical resonator was observed by coupling to an off-chip tank circuit [9]; however, the coupling was not sufficient to observe graphene thermal motion, not to mention cavity backaction.

In this work we make the first demonstration of radiation pressure effects on the motion of graphene in the context of cavity optomechanics. Cooled in a dilution refrigerator, we study the lowest drumlike flexural mode of a bilayer graphene resonator at $\omega_m/2\pi = 24$ MHz, coupled to a high-Q microwave cavity resonator. We observe thermal motion down to 70 mK; furthermore, we carry out cavity backaction sideband cooling to further dampen the effective mode temperature down to 60 mK. A thermal transport model is developed to explain the findings.

The interaction of a mechanical resonator with a microwave-regime electrical cavity is similar to the radiation pressure force; displacement x affects the cavity frequency ω_c. This is naturally described in terms of an equivalent capacitance C of the cavity, and a movable capacitance C_g of the conductive mechanical part. The coupling energy, that is, how much the zero-point motion x_{zp} displaces the cavity frequency, is given by $g = (\omega_c/2C)(\partial C_g/\partial x)x_{\mathrm{zp}}$. Since for a plate capacitor $\partial C_g/\partial x \propto x^{-2}$, a narrow vacuum gap d is instrumental for obtaining a high g.

We have developed a technique to fabricate narrow gaps $d \sim 70$ nm for a membrane about 2.5 μm long and 1.5 μm wide in a bridge geometry. First, high-quality tape-exfoliated bilayer graphene pieces are located on a silicon substrate covered with 275 nm thick SiO_2 and confirmed with Raman spectroscopy. After the lithography and transfer process illustrated in Fig. 1, the gold contact is punched down well in touch to the other end of the aluminum cavity over an area of $\sim 8 \times 3$ μm. The graphene is suspended on top of the opposite end. Since we have a good control of the thickness of the aluminum electrode $d_{\mathrm{Al}} = 80$ nm as well as that of the PMMA stamp $d_{\mathrm{PMMA}} = 150$ nm, the vacuum gap is determined as $d = d_{\mathrm{PMMA}} - d_{\mathrm{Al}} = 70$ nm.

Although the punch from gold to the Al cavity breaks the native oxide on top of Al, a galvanic contact between Au and Al is not established since the Al immediately oxidizes. Hence, the graphene is electrically floating. However, the capacitance C_p between Au and Al satisfies $C_p \gg C_g(x)$ such that the coupling is fully determined by the movable capacitance $C_g(x)$ [see Fig. 2(b) and Ref. [10]]. We expect

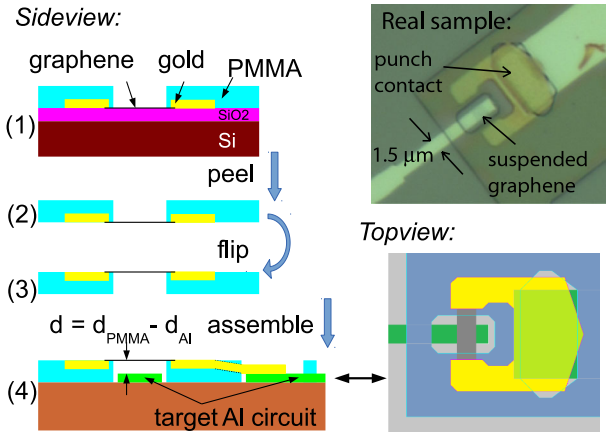

FIG. 1 (color online). Device fabrication. Gold contacts 30 nm thick are deposited on the previously located graphene pieces by e-beam lithography and lift-off. Then PMMA is spun on the chip again and a second e-beam lithography step is applied (1) to define patterns such as stamps and holes in it. The whole PMMA membrane is then peeled off from the initial substrate (2) by etching away the SiO_2 in 1% HF solution. We pick up one of such stamps, flip and transfer it (3)–(4) over the aluminum electrode (one end of the cavity) to form a parallel plate capacitor.

the charge density of the graphene to be low and its resistance thus to be high $R_g \sim 1, \ldots, 10$ kΩ.

The cavity is a mm-size meandering $\lambda/2$ design made out of aluminum on a high-purity silicon chip [Fig. 2(a)]. Since both ends of the cavity are floating, the effective capacitance C in the circuit schematics [Fig. 2(b)] is very low given the dimensions, $C \simeq 45$ fF. We can convert the real circuit in Fig. 2(b) into an equivalent parallel resonator [Fig. 2(c)] where the graphene resistance is included in $R_g' \simeq 1/(\omega_c^2 C_g^2 R_g) \gg R_g$. With the current parameters $C_g, C_{ci}, C_{co} \ll C$, the effective capacitance essentially equals C.

From the parameters of the graphene and the cavity, we obtain a prediction [10] for the coupling of the lowest flexural mode $g/2\pi \simeq 70$ Hz. However, the data are best fitted (see below) by clearly lower $g/2\pi = (35 \pm 8)$ Hz. We attribute this to a tendency of the membrane mode shape to be distorted by nonuniform strain at the clamps.

The measurements are carried out in a dilution refrigerator down to the 22 mK base temperature. We measure transmission of near-resonant microwaves through the cavity [10]. The cavity linewidth below 350 mK is found as $\kappa/2\pi = (5.6 \pm 0.6)$ MHz. This is set by the effective resistance $R_g' \sim 1$ MΩ of the graphene [Fig. 2(c)], thus adding a new dominant loss channel. This finding is consistent with about $1, \ldots, 5$ kΩ total resistance of the graphene.

The information on the mechanical resonator appears in the motional sidebands spaced $\pm\omega_m$ about the pump frequency. We apply the pump microwave irradiation at the "red" detuning frequency $\omega_P = \omega_c - \omega_m$. In Fig. 3(a) we show results for such a measurement which depict the thermal motion of the lowest mode of the suspended graphene. We used such low pump power that the cavity backaction damping (see below) had a negligible effect. The mechanical Q value at the base temperature was about 15×10^3. The corresponding damping rate is $\gamma_m = \omega_m/Q \simeq (2\pi) \times 1.6$ kHz.

As clear in Fig. 3(a), the height of the peaks grows with temperature. Ideally, the peak area is linearly proportional to cryostat temperature T_0, since by equipartition, $1/2 m_{\rm eff}\omega_m^2 \langle x^2 \rangle = 1/2 k_B T_0$. We follow the usual practice and calibrate the transduction between peak area and phonon number by relying on the linear temperature dependence, here obeyed above about $T_0 = 70$ mK as seen in Fig. 3(b). We thus conclude that the lowest flexural mode thermalizes down to 70 mK in this experiment. This represents phonon occupancy 3 orders of magnitude lower than previous observations of graphene thermal motion, made at room temperature [4].

Sideband cooling owing to the radiation pressure interaction has been an extremely powerful and popular tool for studying micromechanical motion [2,3,12–15]. Here, the pump microwave has to be applied at the red sideband, $\omega_P = \omega_c - \omega_m$. This pump condition is similar to that used in the mere detection of the thermal motion as in Fig. 3, but now the pump power is orders of magnitude stronger.

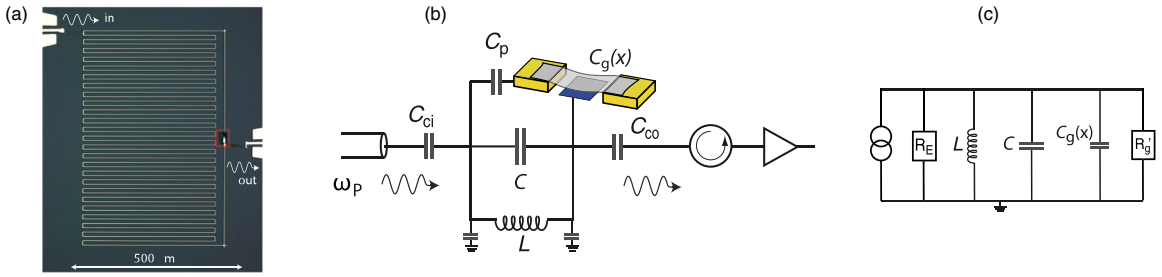

FIG. 2 (color online). Schematic of the experiment. (a) The microwave cavity resonant at 7.8 GHz. White is Al film, 80 nm thick; dark is Si substrate. (b) Scheme of the transmission measurement. The signal couples through the input and output coupling capacitors C_{ci} and C_{co}, respectively. The output signal is amplified at the 4 K stage by a low-noise microwave amplifier, and detected at room temperature by a spectrum analyzer. (c) Equivalent circuit of the cavity including graphene. The resistor R_E marks the losses in the 50 Ω external circuit.

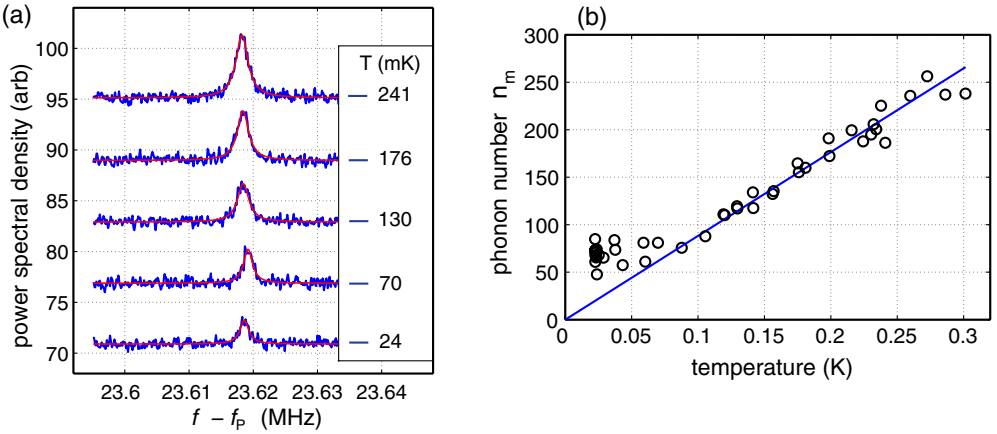

FIG. 3 (color online). Thermal motion of graphene. (a) Spectral density near the motional sideband corresponding to the lowest flexural mode. The curves are shifted vertically for clarity by 6 units. The red lines are Lorentzian fits. (b) Measured phonon number (circles) at different cryostat temperatures. There are several data points nearly on top of each other at 22 mK. The solid line is a least-squares fit to the data above 100 mK. In both (a) and (b), the pump power was about 5 nW, inducing a cavity photon number $n_c \sim 6 \times 10^4$ at ω_p.

The sideband cooling process results in an enhanced effective damping experienced by the mechanical mode [10,16]: $\gamma_{\rm eff} = \gamma_m + \gamma_{\rm opt}$, where $\gamma_{\rm opt} = 4g^2 n_c/\kappa$. The total damping then gives a reduced phonon occupation: $n_m = \gamma_m n_m^T/\gamma_{\rm eff}$. Here, the thermal phonon number n_m^T is set by the bath at the temperature $T_{\rm env}$ according to $\hbar\omega_m n_m^T = k_B T_{\rm env}$. Although ideally the bath equilibrates at the cryostat temperature, in the following we find that the microwave heating causes that $T_{\rm env} \gg T_0$.

In the measurement, we indeed observe the thermal motion peak becoming broader as the pump power is increased [Fig. 4(a)]. This is found to be in good agreement to the prediction from a pure microwave radiation pressure interaction between the cavity and graphene, displayed in

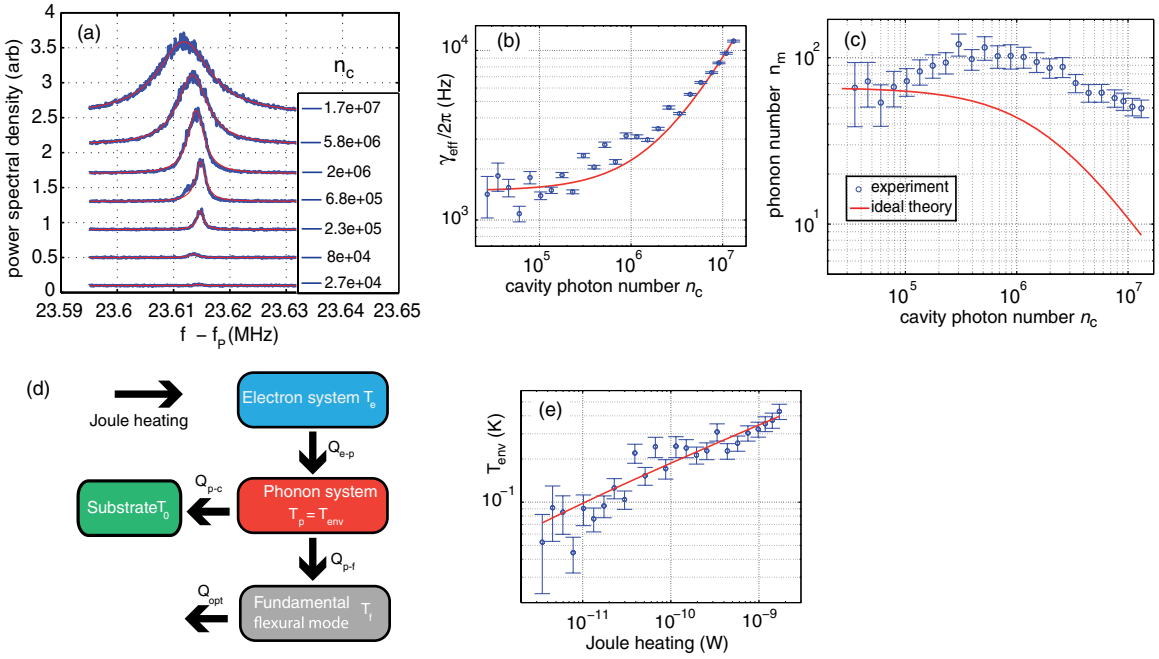

FIG. 4 (color online). Cooling and heating. (a) Thermal motion spectra representing progressing sideband cooling at increasing cavity pump photon occupancies. The curves have been shifted vertically for clarity. The red lines are Lorentzian fits. (b) Total damping rate of the graphene resonance versus cavity photon number. The solid line is a fit to theory. (c) Phonon number of the graphene mechanical mode versus pump occupancy. The solid line is the ideal behavior. (d) Thermal model used to describe microwave heating. (e) Effective temperature of the environment of the mechanical mode versus power dissipation in the graphene, related to pump occupancy. The solid line is a T^4 fit.

Fig. 4(b). The slight deviation around $n_c \sim 5 \times 10^5$ is probably due to an intermittent two-level fluctuation, occurring at n_c values in this range, of the graphene frequency between two values spaced by about 300 Hz. This effect, not occurring at other values of n_c, is seen in the middle curve in Fig. 4(a) as a doubling of the peak.

At the same time as the peaks widen in Fig. 4(a), the height of the peaks grow progressively larger, although according to an ideal theory, the peaks should become lower above $n_c \sim 10^6$. We attribute this to an enhanced temperature of the environment experienced by the graphene mechanical mode. We can first extract the phonon number n_m from the Lorentzians in Fig. 4(a), showing progress of the sideband cooling in Fig. 4(c). The cooling process clearly deviates from the ideal picture, and shows the unusual nonmonotonic behavior. Knowing n_m and $\gamma_{\rm opt}$, we can also deduce the environmental phonon number n_m^T [Fig. 4(e)]. A relatively weak dependence of the temperature on microwave power hints that there is a strongly temperature-dependent bottleneck setting the contact of the flexural mode to its bath.

We can describe the mode temperature with a thermal model [Fig. 4(d)] of the chip at a cryostat temperature T_0. We start by supposing the graphene electrons heat by Joule heating by microwave currents. Because the graphene is electrically floating, heat flow out from the electrons $\dot{Q}_{e-p}$ is entirely due to electron-phonon coupling. The phonons are scattered into the substrate across the relatively large contact area, the corresponding heat flow being $\dot{Q}_{p-c}$. We also suppose the thermal environment of the lowest flexural mode is set by the phonon bath which couples via mechanical nonlinearities. The mode temperature is also affected by the sideband cooling with heat flow $\dot{Q}_{\rm opt}$. In a typical case here, $\dot{Q}_{\rm opt} \ll \dot{Q}_{p-c}$.

We review the theory of the electron-phonon coupling [17–20] in the Supplemental Material [10]. The quantity of interest, the phonon temperature, is bottlenecked by the Kapitza thermal boundary resistance between the graphene and gold. The present experiment allows for accurate measurement of this important quantity, not performed previously in dilution refrigerator temperatures. The data in Fig. 4(e) are fitted as $\dot{Q}_{p-c} = A_c R_K (T_p^4 - T_0^4)$, where the Kapitza conductivity $R_K = (0.4 \pm 0.1) \times 10^4$ W K^{-4} m^{-2}, and $A_c \simeq 9$ μm^2 is the contact area. At the largest electronic heating of 3.5 nW [Fig. 4(e)], the weak electron-phonon coupling results in $T_e = 10$ K.

For 3D systems the following temperature dependence for the Kapitza conductivity is expected: $\dot{Q}_{p-c} = A_c R_K (T_p^4 - T_0^4)$. In thin films, the density of phonon modes is different, and often an exponent between 3 and 4 is observed [21]. In graphene-metal systems, the temperature dependence of R_K has been determined down to ~50 K [22,23] but not below; similar values have been obtained for graphene-SiO_2 interfaces [24] but there coupling to interfacial modes has been found to be important as well [25]. Consequently, only rather crude estimates are available: we employ the results of Refs. [22,24], extended by a diffuse mismatch model [26] to the asymptotic region with T^4 dependence. This yields for Kapitza conductance values that are 2 orders of magnitude smaller than that obtained from fitting to Fig. 4(e) but much larger than the electron-phonon coupling. Hence, the graphene-substrate thermal contact seems better than expected from theory. This can be partially due to conduction through Au.

It is intriguing to further estimate the prospect of ground-state cooling, quantified usually as $n_m < 1$, of the mechanical modes of graphene relying on microwave radiation pressure. By an increase of coupling g one obtains, at a given bath temperature set by pump strength n_c, higher damping and thus more efficient cooling. We obtain [10] that a coupling $g/2\pi \simeq 600$ Hz would be enough to cool to the ground state in the present setting using a bilayer graphene. This is achieved by a narrower vacuum gap $d = 35$ nm, and by reducing the cavity capacitance down to $C \sim 20$ fF by using low-dielectric substrate such as quartz [27]. A monolayer graphene or higher mechanical Q value will clearly alleviate these requirements. Another possibility is to add a voltage gate for tuning the graphene charge density which sensitively affects the Joule heating and thus only a modest increase in coupling is needed. These values are not immediately at hand but are realistic, and hence we believe we can obtain the required coupling and reach the quantum ground state of moving graphene in the near future.

Our work has brought together two timely topics: graphene and cavity optomechanics. This will open up new directions owing to the large zero-point motion, large mechanical nonlinearity even at the few-quantum level [28–30], or along the interplay [31,32] of traditional graphene physics and mechanics.

We thank Erno Damskägg, Tero Heikkilä, and Juha Pirkkalainen for useful discussions. This work was supported by the Academy of Finland (CoE and 259912), by the European Research Council (240387-NEMSQED), and by FP7 Grant No. 323 924 iQUOEMS, and partially by Graphene Flagship. The work benefited from the facilities at the Micronova Nanofabrication Center and at the Low Temperature Laboratory infrastructure.

*Mika.Sillanpaa@aalto.fi

[1] T. J. Aspelmeyer, M. Kippenberg, and F. Marquardt, arXiv:1303.0733 [Rev. Mod. Phys. (to be published)].
[2] J. D. Teufel, T. Donner, D. Li, J. W. Harlow, M. S. Allman, K. Cicak, A. J. Sirois, J. D. Whittaker, K. W. Lehnert, and R. W. Simmonds, Nature (London) **475**, 359 (2011).
[3] J. Chan, T. P. M. Alegre, A. H. Safavi-Naeini, J. T. Hill, A. Krause, S. Gröblacher, M. Aspelmeyer, and O. Painter, Nature (London) **478**, 89 (2011).

[4] J. S. Bunch, A. M. van der Zande, S. S. Verbridge, I. W. Frank, D. M. Tanenbaum, J. M. Parpia, H. G. Craighead, and P. L. McEuen, Science **315**, 490 (2007).
[5] D. Garcia-Sanchez, A. M. van der Zande, A. S. Paulo, B. Lassagne, P. L. McEuen, and A. Bachtold, Nano Lett. **8**, 1399 (2008).
[6] Y. Xu, C. Chen, V. V. Deshpande, F. A. DiRenno, A. Gondarenko, D. B. Heinz, S. Liu, P. Kim, and J. Hone, Appl. Phys. Lett. **97**, 243111 (2010).
[7] S. Lee, C. Chen, V. V. Deshpande, G.-H. Lee, I. Lee, M. Lekas, A. Gondarenko, Y.-J. Yu, K. Shepard, P. Kim *et al.*, Appl. Phys. Lett. **102**, 153101 (2013).
[8] R. A. Barton, I. R. Storch, V. P. Adiga, R. Sakakibara, B. R. Cipriany, B. Ilic, S. P. Wang, P. Ong, P. L. McEuen, J. M. Parpia *et al.*, Nano Lett. **12**, 4681 (2012).
[9] X. Song, M. Oksanen, M. A. Sillanpää, H. G. Craighead, J. M. Parpia, and P. J. Hakonen, Nano Lett. **12**, 198 (2012).
[10] See Supplemental Material at http://link.aps.org/supplemental/10.1103/PhysRevLett.113.027404 for details of the experiment and modeling, which includes Ref. [11].
[11] I. W. Frank, D. M. Tanenbaum, A. M. van der Zande, and P. L. McEuen, J. Vac. Sci. Technol. B **25**, 2558 (2007).
[12] S. Gigan, H. R. Boehm, M. Paternostro, F. Blaser, G. Langer, J. B. Hertzberg, K. C. Schwab, D. Baeuerle, M. Aspelmeyer, and A. Zeilinger, Nature (London) **444**, 67 (2006).
[13] A. Schliesser, O. Arcizet, R. Riviere, G. Anetsberger, and T. J. Kippenberg, Nat. Phys. **5**, 509 (2009).
[14] T. Rocheleau, T. Ndukum, C. Macklin, J. B. Hertzberg, A. A. Clerk, and K. C. Schwab, Nature (London) **463**, 72 (2010).
[15] F. Massel, S. U. Cho, J.-M. Pirkkalainen, P. J. Hakonen, T. T. Heikkilä, and M. A. Sillanpää, Nat. Commun. **3**, 987 (2012).
[16] F. Marquardt, J. P. Chen, A. A. Clerk, and S. M. Girvin, Phys. Rev. Lett. **99**, 093902 (2007).
[17] E. McCann, Phys. Rev. B **74**, 161403 (2006).
[18] J. K. Viljas and T. T. Heikkilä, Phys. Rev. B **81**, 245404 (2010).
[19] D. K. Efetov and P. Kim, Phys. Rev. Lett. **105**, 256805 (2010).
[20] J. Yan, M.-H. Kim, J. A. Elle, A. B. Sushkov, G. S. Jenkins, H. M. Milchberg, M. S. Fuhrer, and H. D. Drew, Nat. Nanotechnol. **7**, 472 (2012).
[21] E. Swartz and R. Pohl, Rev. Mod. Phys. **61**, 605 (1989).
[22] A. J. Schmidt, K. C. Collins, A. J. Minnich, and G. Chen, J. Appl. Phys. **107**, 104907 (2010).
[23] A. A. Balandin, Nat. Mater. **10**, 569 (2011).
[24] Z. Chen, W. Jang, W. Bao, C. N. Lau, and C. Dames, Appl. Phys. Lett. **95**, 161910 (2009).
[25] M. Freitag, M. Steiner, Y. Martin, V. Perebeinos, Z. Chen, J. C. Tsang, and P. Avouris, Nano Lett. **9**, 1883 (2009).
[26] J. C. Duda, J. L. Smoyer, P. M. Norris, and P. E. Hopkins, Appl. Phys. Lett. **95**, 031912 (2009).
[27] F. Massel, T. T. Heikkilä, J.-M. Pirkkalainen, S. U. Cho, H. Saloniemi, P. J. Hakonen, and M. A. Sillanpää, Nature (London) **480**, 351 (2011).
[28] J. Atalaya, A. Isacsson, and J. M. Kinaret, Nano Lett. **8**, 4196 (2008).
[29] M. A. Sillanpää, R. Khan, T. T. Heikkilä, and P. J. Hakonen, Phys. Rev. B **84**, 195433 (2011).
[30] A. Voje, J. M. Kinaret, and A. Isacsson, Phys. Rev. B **85**, 205415 (2012).
[31] V. Singh, B. Irfan, G. Subramanian, H. S. Solanki, S. Sengupta, S. Dubey, A. Kumar, S. Ramakrishnan, and M. M. Deshmukh, Appl. Phys. Lett. **100**, 233103 (2012).
[32] M. V. Medvedyeva and Y. M. Blanter, Phys. Rev. B **88**, 125423 (2013).